JACS Au
AN OPEN ACCESS JOURNAL OF THE AMERICAN CHEMICAL SOCIETY

pubs.acs.org/jacsau
Letter

Total Synthesis of (−)-Elodeoidins A and B

Chungwoo Lee, Gyumin Kang, Jaehyun You, Taewan Kim, Hee-Seung Lee, Yoonsu Park,* and Sunkyu Han*

Cite This: *JACS Au* 2025, 5, 1096−1103
Read Online
ACCESS | Metrics & More | Article Recommendations | Supporting Information

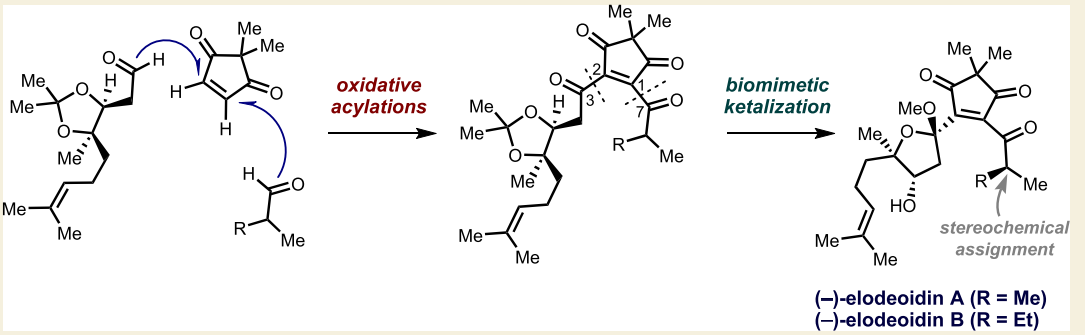

ABSTRACT: Biomimicry has long been a valuable approach for designing efficient synthetic strategies in complex natural product synthesis. However, abiotic yet powerful transforms can significantly streamline the synthesis by introducing greater convergence to the synthetic route. Herein, we delineate a convergent total synthesis of elodeoidins A and B, enabled by a cross-dehydrogenative coupling (CDC) reaction between an aldehyde and an electron-deficient olefin. The CDC reaction operating under the newly discovered reaction conditions proceeds via distinct concerted deprotonation within the formal Cu(III) catalytic complex. Furthermore, the total synthesis of both structural candidates of elodeoidin B revealed that the natural product exists as a mixture of epimers at the C8 stereocenter.

KEYWORDS: *total synthesis, cross-dehydrogenative coupling, polycyclic polyprenylated acylphloroglucinols, reaction mechanism, elodeoidins*

Hypericum elodeoides, a traditional medical herb that has been used to treat stomatitis, infantile pneumonia, and mastitis in China, is recognized as a rich source of various polycyclic polyprenylated acylphloroglucinols (PPAPs),[1,2] acylphloroglucinol meroterpenoids,[3] and their derivatives.[4] This family of natural products has inspired the development of novel synthetic strategy and tactics.[5−8] In 2021, Kong and co-workers isolated a new family of natural products, elodeoidins A−H (**1**−**8**) from the same plant species (Figure 1).[9] The distinct structural feature of these natural products compared to the more conventional acylphloroglucinol meroterpenoids is the presence of a five-membered *β*-diketone moiety with a *gem*-dimethyl group.

The isolation team proposed that elodeoidins A (**1**) and B (**2**) are biosynthesized from tetraketone precursor **9** via a sequence involving oxidation, hemiketalization, and methylation (Scheme 1). The five-membered diketone moiety in **9** was proposed to be forged by an *α*-ketol rearrangement of precursor **10**. Presumed precursor **10** was suggested to be derived from an oxidation of acylfilicinic acid derivative **11** derived from acylphloroglucinol.[10]

Fascinated by the structure of elodeoidins, we sought to establish a synthetic route to these natural products. While

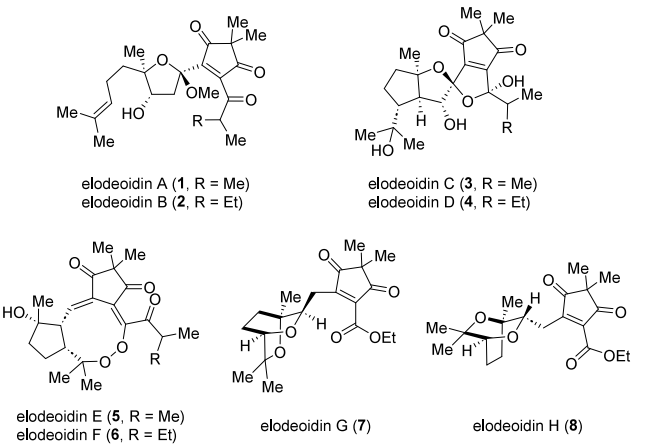

Figure 1. Elodeoidin natural products.

Received: February 19, 2025
Revised: February 26, 2025
Accepted: February 28, 2025
Published: March 12, 2025

Scheme 1. Comparison between Retrobiosynthetic and Retrosynthetic Analysis of Elodeoidins A and B

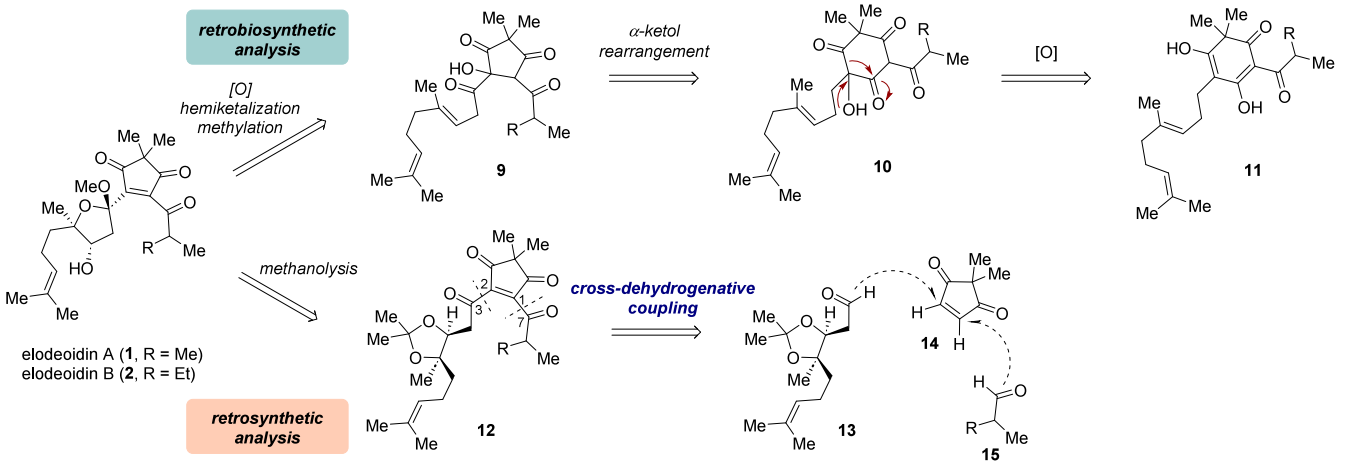

biomimicry can guide the invention of novel synthetic strategies,[11−17] in the case of elodeoidins A (**1**) and B (**2**), we envisioned that cross-dehydrogenative coupling (CDC) reaction between an aldehyde and an electron-deficient olefin would significantly streamline the synthesis of the target molecules. CDC reactions have demonstrated their utility in constructing functional molecules via direct activation of C−H bonds under oxidative conditions.[18,19] However, there are only a few published examples of intermolecular CDC reactions between aldehydes and electron-deficient olefins.[20−23] Recently, our group reported the development of Cu-catalyzed CDC reaction between an aldehyde and an electron-deficient olefin and its application into the synthesis of flueggeacosine B.[24,25] From a retrosynthetic perspective, we aimed to synthesize elodeoidins A (**1**) and B (**2**) through methanolysis of intermediate **12**. This intermediate was planned to be accessed by forming the key C2−C3 and C1−C7 bonds through two successive CDC reactions involving enedione **14** and aldehydes **13** and **15** (Scheme 1).

We initiated our studies by exploring the C−C bond formation between aldehyde **16** and 2,2-dimethyl-4-cyclopentene-1,3-dione (**14**) or its derivatives **17**. To accomplish this, we first approached it using classical methods such as the Baylis−Hillman reaction (Table 1, entry 1), Nozaki−Hiyama−Takai−Kishi coupling (Table 1, entry 2), and Stetter reaction (Table 1, entry 3). Unfortunately, all these approaches were unsuccessful, resulting in the decomposition of the substrates.

We then turned our attention to the visible-light-mediated Cu-catalyzed CDC reaction previously developed by our group.[24] Direct coupling between isobutyraldehyde (**16**) and 2,2-dimethyl-4-cyclopentene-1,3-dione (**14**) using Cu(dap)$_2$Cl,[26] *tert*-butyl-peroxy 2-ethylhexylcarbonate (TBEC), quinuclidine, and quinuclidine hydrochloride under 525 nm light irradiation did not show any reactivity (Table 1, entry 4). To remedy this problem, the chloride moiety was introduced at the α-position of the enedione substrate.[27] DFT calculations revealed that the LUMO energy level of chlorinated enedione **17b** was 0.262 eV lower than that of enedione **14** (see Supporting Information for details). To our pleasure, the CDC reaction between **16** and **17b** under the aforementioned reaction conditions afforded the desired product **21** in 70% yield (Table 1, entry 5). However, derivatizing chloride **21** for subsequent C−C bond formation proved challenging (see Supporting Information for details).

Table 1. Attempted Approaches for the Acylation of Compounds 14 and 17

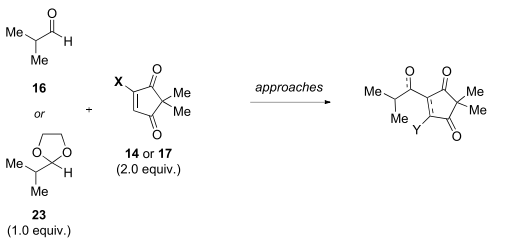

Entry	Approaches	X (compound)	Expected product	Result
1	Baylis−Hillman type reaction[a]	H (**14**)	**18**	complex mixture
2	Nozaki−Hiyama−Takai−Kishi coupling[b]	Br (**17a**)	**19**	decomposition
3	Stetter-type reaction[c]	Cl (**17b**)	**20**	decomposition
4	Cross-dehydrogenative coupling[d]	H (**14**)	**20**	no reaction
5	Cross-dehydrogenative coupling[d]	Cl (**17b**)	**21**	70%
6	Cross-dehydrogenative coupling[e,f]	H (**14**)	**22**	48%

[a]Reagents and conditions are as follows: [a] DABCO (1.2 equiv), pyrrolidine (1.2 equiv), $NaHCO_3$ (1.2 equiv), THF, 23 °C; [b] $NiCl_2$ (5 mol %), $CrCl_2$ (5.0 equiv) DMF, 50 °C; [c] 3-Benzyl-5-(2-hydroxyethyl)-4-methylthiazolium chloride (50 mol %), triethylamine (2.0 equiv), 1,4-dioxane, 50 °C; [d] Cu(dap)$_2$Cl (0.05 mol %), *tert*-butyl-peroxy 2-ethylhexylcarbonate (2.0 equiv), quinuclidine (20 mol %), quinuclidine hydrochloride (20 mol %), MeCN, 23 °C, 525 nm. [e] Reaction carried out with 2-isopropyl-1,3-dioxolane (**23**) instead of isobutyraldehyde (**16**) [f] Cu(dap)$_2$Cl (5 mol %) *tert*-butyl-peroxy 2-ethylhexylcarbonate (2.0 equiv), quinuclidine (20 mol %), MeCN, 23 °C, 525 nm.

Alternatively, we envisioned that the acetal derivative of **16** could serve as a plausible coupling partner for the CDC

https://doi.org/10.1021/jacsau.5c00201
JACS Au 2025, 5, 1096−1103

reaction. DFT calculation showed that the SOMO energy level of α,α-dialkoxy radical from 2-isopropyl-1,3-dioxolane (**23**) was 1.021 eV higher than that of the acyl radical derived from **16** (see the Supporting Information for details). Delightfully, when dioxolane **23** and enedione **14** were subjected to the $Cu(dap)_2Cl$-catalyzed CDC reaction conditions, product **22** was obtained in 48% yield (Table 1, entry 6).

Based on these observations, we designed acetal **27** as a plausible CDC partner of enedione **14** for the synthesis of elodeoidins A (**1**) and B (**2**). The synthesis of dioxolane **27** commenced from aldehyde **24**, previously synthesized by the Yamano group in six steps from geraniol (Scheme 2).[28] Wittig

Scheme 2. Initial Synthetic Route towards Elodeoidin A[a]

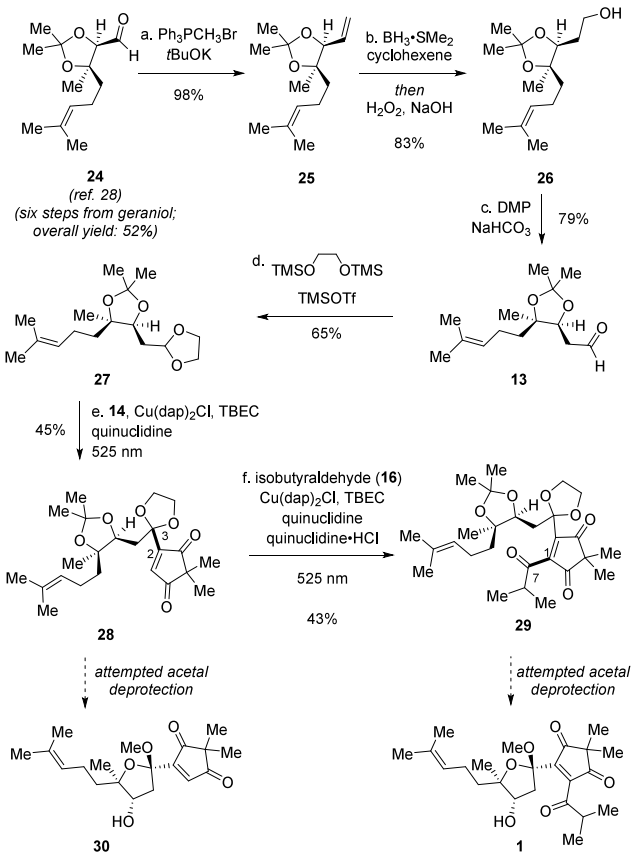

[a]Reagents and conditions are as follows: [a] Ph_3PCH_3Br (2.0 equiv), *t*BuOK (3.0 equiv), THF, 0 to 23 °C, 98%; [b] $BH_3{\cdot}SMe_2$ (1.5 equiv), cyclohexene (3.0 equiv), THF, 0 to 23 °C then add H_2O_2, NaOH, 0 °C, 83%; [c] DMP (2.0 equiv), $NaHCO_3$ (3.0 equiv), CH_2Cl_2, 0 to 23 °C, 79%; [d] 1,2-bis(trimethylsiloxyethane) (6.0 equiv), TMSOTf (75 mol %), CH_2Cl_2, −30 °C, 65%; [e] **14** (10 equiv), $Cu(dap)_2Cl$ (1.0 mol %), TBEC (2.0 equiv), quinuclidine (20 mol %), MeCN, 23 °C, 525 nm, 45%; [f] **16** (2 equiv), $Cu(dap)_2Cl$ (1.0 mol %), TBEC (2.0 equiv), quinuclidine (20 mol %), quinuclidine hydrochloride (20 mol %), MeCN, 23 °C, 525 nm, 43%.

olefination of **24** with the ylide produced from methyltriphenylphosphonium bromide and potassium *tert*-butoxide resulted in terminal olefin **25** in 98% yield. Regioselective hydroboration with dicyclohexylborane and subsequent oxidation with hydrogen peroxide yielded primary alcohol **26** in 83% yield. Dess−Martin periodinane oxidized the primary alcohol moiety of **26** to furnish aldehyde **13** in 79% yield. The transformation of aldehyde **13** to dioxolane **27** was achieved in the presence of 1,2-bis(trimethylsiloxy)ethane and trimethylsilyl triflate in 65% yield.[29]

With solid access to dioxolane **27**, we next investigated the key CDC reaction. When dioxolane **27** and enedione **14** were allowed to react with $Cu(dap)_2Cl$, TBEC, and quinuclidine in acetonitrile under green light irradiation (525 nm), the C2−C3 coupled product **28** was obtained in 45% yield (Scheme 2). Subsequent conjugation between **28** and isobutyraldehyde (**16**) cultivated the C1−C7 coupled product **29** in 43% yield under the established CDC reaction conditions.[24] Compound **29** consists of all C−C bonds present in elodeoidin A (**1**). The remaining steps were the global deprotection of acetals and in situ hemiketalization. However, despite numerous attempts using various Brønsted and Lewis acids, the methanolysis or hydrolysis of acetal **29** was unsuccessful, with the acetal moiety remained intact in most cases. Efforts to deprotect the acetal moiety of compound **28** also proved problematic (see Supporting Information for details on the deprotection conditions tested for **28** and **29**). The difficulties encountered with acid-mediated hydrolysis of **28** and **29** prompted us to explore an alternative synthetic approach for our target compounds.

As an alternative approach for the acylation of enedione **14** with the aldehyde substrate, we envisioned a sequence involving radical-mediated hydroacylation and subsequent oxidation. Gratifyingly, when enedione **14** was allowed to react with isobutyraldehyde (**16**) in the presence of tetrabutylammonium decatungstate (TBADT) under 370 nm light irradiation,[30,31] conjugated intermediate **31** was obtained in its enol form (Scheme 3). Subsequent treatment of **31** with phenylselenyl chloride and pyridine, followed by oxidation with hydrogen peroxide, afforded enetrione **20** in 68% yield over 2 steps.

Scheme 3. Total Synthesis of (−)-Elodeoidin A[a]

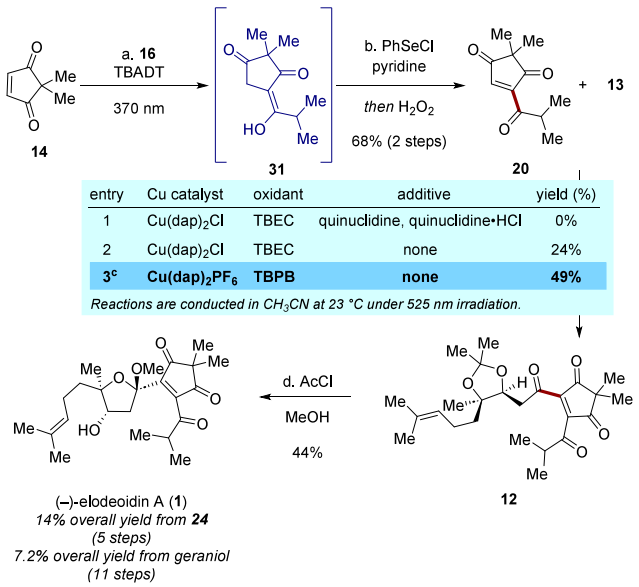

entry	Cu catalyst	oxidant	additive	yield (%)
1	$Cu(dap)_2Cl$	TBEC	quinuclidine, quinuclidine•HCl	0%
2	$Cu(dap)_2Cl$	TBEC	none	24%
3[c]	$Cu(dap)_2PF_6$	TBPB	none	49%

Reactions are conducted in CH_3CN at 23 °C under 525 nm irradiation.

[a]Reagents and conditions are as follows: [a] **16** (5.0 equiv), TBADT (5 mol %), MeCN, 23 °C, 370 nm; [b] PhSeCl (1.1 equiv), pyridine (1.2 equiv), CH_2Cl_2, 23 °C then H_2O_2, 68% (2 steps); [c] **13** (1.0 equiv), **20** (2.0 equiv), $Cu(dap)_2PF_6$ (0.1 mol %), TBPB (2.0 equiv), MeCN, 23 °C, 525 nm, 49%; [d] AcCl (cat.), MeOH, 0 to 23 °C, 44%.

https://doi.org/10.1021/jacsau.5c00201
JACS Au 2025, 5, 1096−1103

Scheme 4. Proposed Reaction Mechanism of Newly Developed CDC Reaction

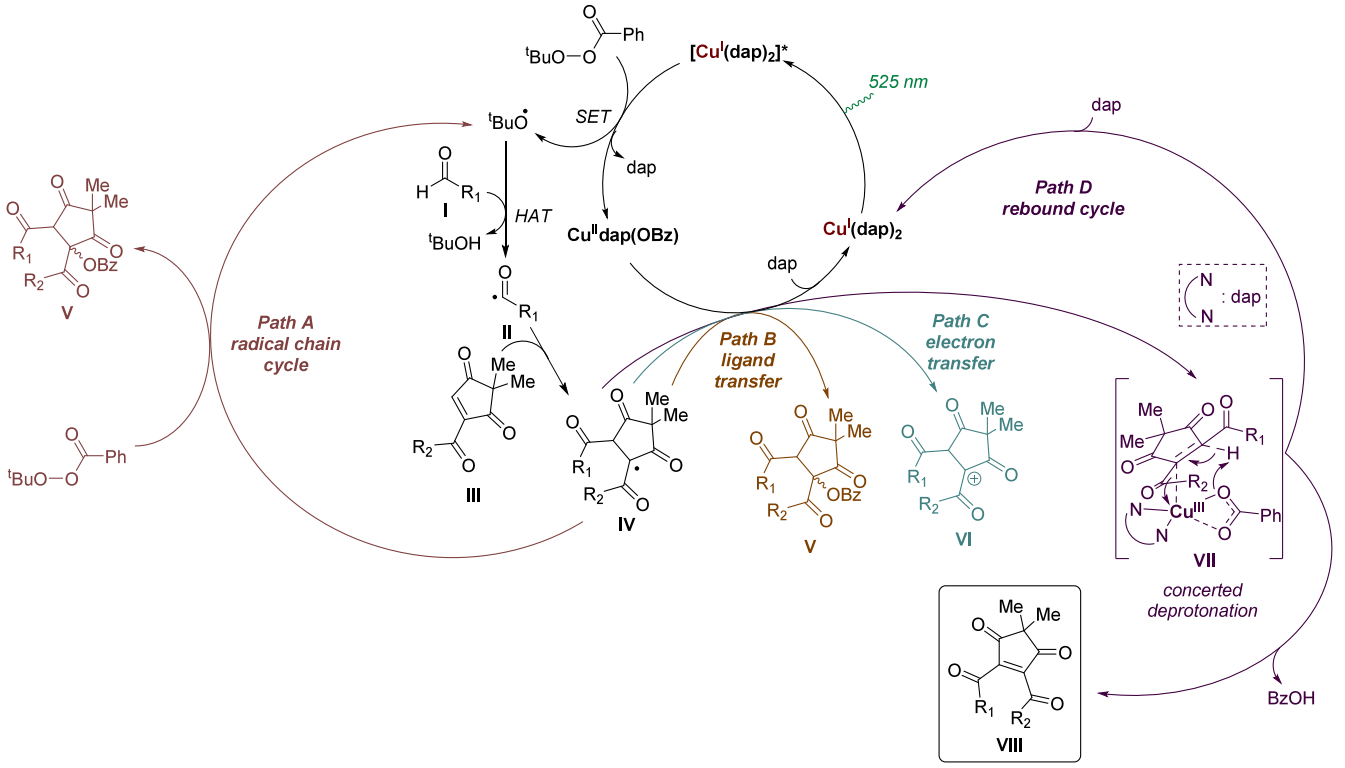

We then attempted the next acylation reaction using the previously described CDC reaction. However, initial attempts of CDC reaction between enetrione **20** and aldehyde **13** under the aforementioned standard reaction conditions[24] did not yield the desired product (Scheme 3). We noticed that the highly electrophilic enetrione **20** was incompatible with nucleophilic quinuclidine. After extensive experimentations, we discovered that the desired product **12** was formed in the absence of quinuclidine and its hydrochloride salt (24% yield). Further optimization studies revealed that $Cu(dap)_2PF_6$ and *tert*-butyl peroxybenzoate (TBPB) are the optimal catalyst and oxidant, respectively, for this transformation, providing the coupled product **12** in 49% yield. Final methanolysis of the acetonide moiety of **12** and hemiketalization of the resulting alcohol intermediate in the presence of a catalytic amount of acetyl chloride in methanol furnished the first synthetic sample of (−)-elodeoidin A (**1**) in 44% yield (14% overall yield from **24** over 5 steps; 7.2% overall yield from geraniol over 11 steps).

It was apparent that the newly discovered reaction conditions for the CDC reaction between **13** and **20** operated through a different mechanism compared to our previously described dual Cu/base catalytic system.[24] We propose that the photoredox cycle is initiated by the visible light-induced excitation of $[Cu(dap)_2]^+$ species, which facilitates the reductive cleavage of the O−O bond in TBPB, leading to the formation of a *tert*-butoxy radical intermediate (Scheme 4). Hydrogen atom transfer (HAT) between the *tert*-butoxy radical intermediate and aldehyde **I** generates nucleophilic acyl radical **II**, which subsequently undergoes a conjugate addition to enetrione **III**, yielding radical intermediate **IV**. At this stage, we initially proposed that radical intermediate **IV** can proceed through multiple potential pathways (pathways A−D).[32,33] In path A, a radical chain mechanism is proposed, wherein radical intermediate **IV** reacts with TBPB to regenerate *tert*-butoxy radical intermediate. Path B involves a ligand transfer from $[Cu(dap)(OBz)]^{2+}$ to intermediate **IV**, leading to the formation of intermediate **V**. In path C, intermediate **IV** undergoes oxidation to generate carbocation **VI** while regenerating Cu(I) from Cu(II) species. Finally, path D consists of a rebound cycle in which radical intermediate **IV** rebinds to $[Cu(dap)(OBz)]^{2+}$, forming a transient formal Cu(III)-alkyl complex **VII**. In this pathway, the final product **VIII** would be obtained after a concerted deprotonation mechanism or a reductive elimination (*vide infra*) within the copper complex, releasing benzoic acid and regenerating the Cu(I) catalyst.

To shed light on the mechanism of our newly developed CDC reaction between an enetrione and an aldehyde, we first measured the quantum yield of the reaction.[34,35] The quantum yield of the CDC reaction between isobutyraldehyde (**16**) and enetrione (**20**) was determined to be 0.054. Even though we cannot completely rule out the possibility of very unproductive radical chain propagation, this observation likely suggests that the catalytic cycle operates within a closed loop without chain propagation (Scheme 5). Furthermore, the light on-and-off experimental results indicated that the radical chain cycle (Scheme 4, path A) is unlikely to be a major pathway in the overall reaction mechanism.

The reaction between dioxolane **33** and electron-deficient olefin **34** with $Cu(dap)_2Cl$ (0.25 mol %), TBEC (1.0 equiv) and quinuclidine hydrochloride (1.2 equiv) in acetonitrile under 525 nm irradiation, the previously reported reaction conditions,[24] yielded *α*-chloroamide **35** in 53% yield (Scheme 5). This result is in agreement with our previously suggested mechanism involving the halide transfer. In stark contrast, when our newly developed CDC reaction conditions, employing $Cu(dap)_2PF_6$ (0.1 mol %) and TBPB (2.0 equiv), were

https://doi.org/10.1021/jacsau.5c00201
JACS Au 2025, 5, 1096−1103

Scheme 5. Experimental Results Regarding the Mechanism of the Newly Discovered CDC Reaction

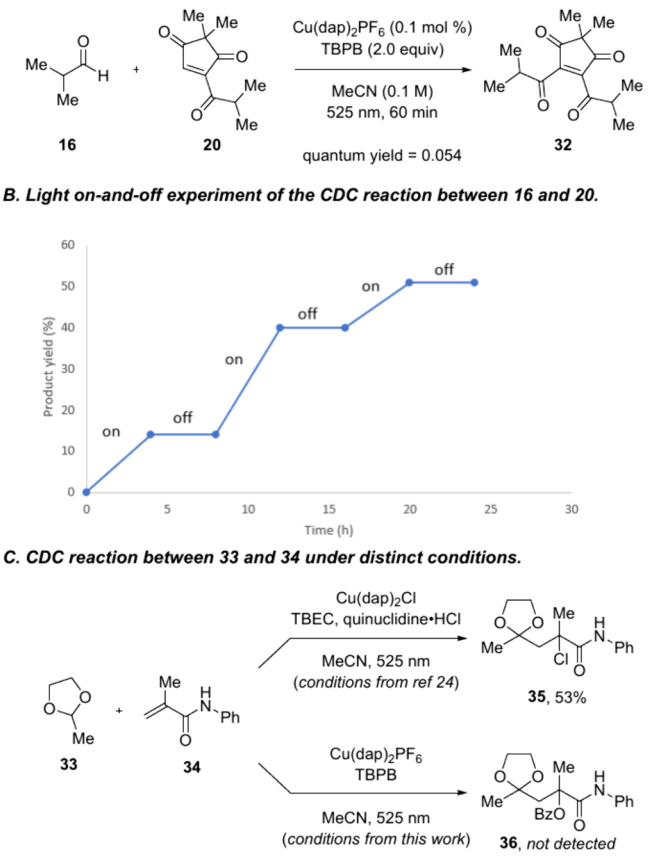

applied to substrates **33** and **34**, product **36** resulting from a ligand transfer was not detected. This observation ruled out the possibility of ligand transfer as a major mechanistic pathway (Scheme 4, path B). Path C is also unlikely to occur due to the instability of α,α'-dicarbonyl cation intermediate **VI** (Scheme 4). Based on these results and previous reports on copper-mediated transformations,[32,33,36−40] we propose that the rebound cycle (Scheme 4, path D) would be the dominant reaction pathway under our reaction conditions.

To gain further insights on the mechanism of the newly discovered reaction conditions, we conducted DFT calculations, including intrinsic bond orbital (IBO) analysis, on the CDC reaction between simpler substrates, enetrione **39** and acetaldehyde (**37**). While the redox potential of the $[Cu(dap)_2]^{+}$*/$[Cu(dap)_2]^{2+}$ couple was reported to be −1.43 V (vs SCE),[41] the reduction peak potential of TBPB was determined to be −1.38 V (vs SCE).[42] Hence, the initial step would involve the reduction of TBPB by the photoexcited $[Cu(dap)_2]^{+}$* to generate $[Cu(dap)(OBz)]^{+}$ and *tert*-butoxy radical intermediate (Scheme 6). *tert*-Butoxy radical species would then abstract hydrogen from acetaldehyde to yield acyl radical **38** with a barrier of 10.40 kcal/mol. Acyl radical **38** would undergo Giese addition to enetrione **39** to form a radical adduct **40**. Radical intermediate **40** would subsequently react with $[Cu(dap)(OBz)]^{2+}$ to generate transient formal Cu(III)−alkyl complex **42**. Notably, the alternative pathway involving single electron transfer from the Cu^{2+} species to radical **40** to form the enolate intermediate **41** turned out to be thermodynamically implausible (51.53 kcal/mol uphill).

The transient Cu^{3+}−alkyl complex **42** would experience an exothermic concerted deprotonation[43−45] to give enetetraone product **44**, benzoic acid, and $[Cu(dap)_2]^{+}$ upon recomplexation with a dap ligand.[46] To further corroborate the electron

Scheme 6. DFT Calculation-Based Energy Level Profile Including IBO Analysis of the Newly Developed CDC Reaction[a]

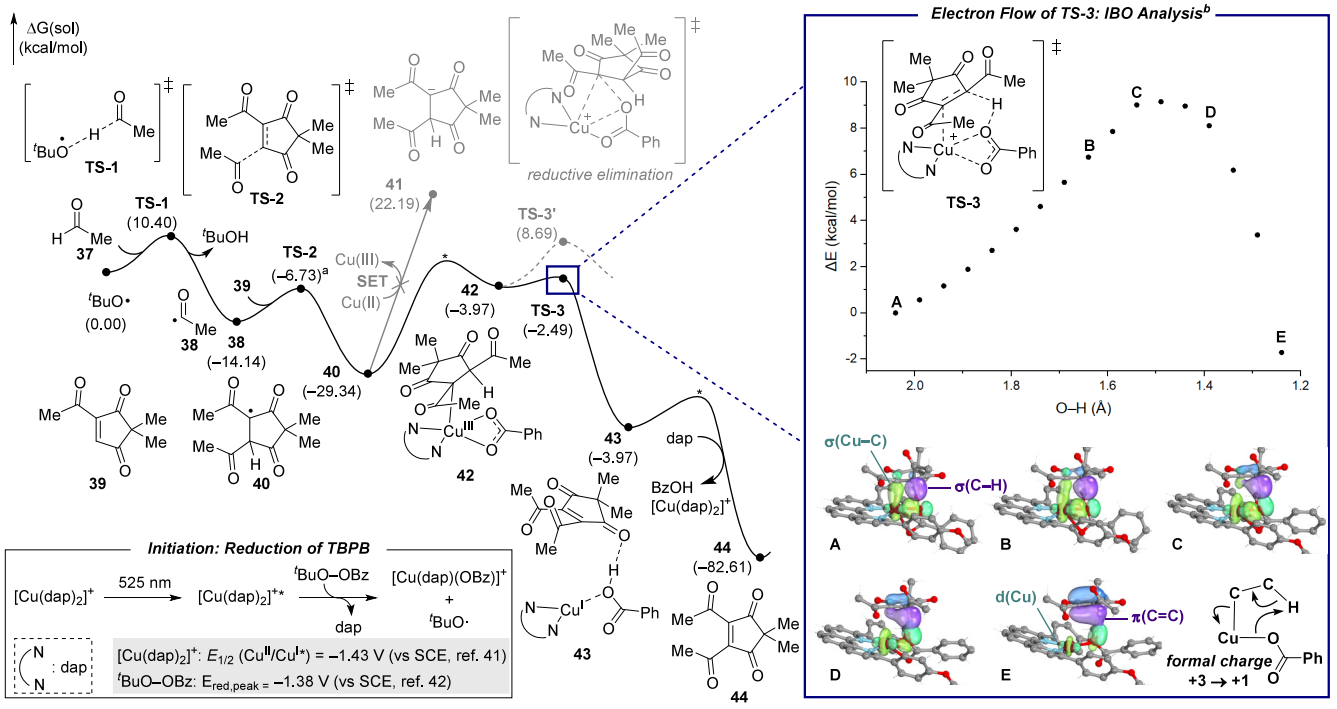

[a]Estimated via solution-phase free energy scan (see Section S8.4 for details). [b]For IBO analysis, orbital energies were re-evaluated by the IBO exponent 2 orbital localization method based on the DFT calculation results in MO6/def2SVP level of theory.

https://doi.org/10.1021/jacsau.5c00201
JACS Au 2025, 5, 1096−1103

flow of the concerted deprotonation step, IBO analysis[47] was performed. As the reaction progresses from point A to point E (Scheme 6), the electron density occupying the σ-orbital of the methine C−H bond flows to form the π-bond. Concurrently, the electron cloud in the Cu−C σ bond flows to the Cu atom, thereby reducing the Cu center, formally from Cu(III) to Cu(I). It is important to note that the reaction pathway involving the reductive elimination of Cu^{3+}−alkyl complex **42** was ruled out due to its higher activation barrier compared to that in the concerted deprotonation pathway (Scheme 6).

We then aimed to complete the total synthesis of elodeoidin B (**2**) and determine the configuration at the C8 stereocenter. While DFT-based predictions of NMR chemical shifts and coupling constants are effective for conformationally rigid molecules,[48−50] the conformational flexibility of both structural candidates, **2a** and **2b**, made such calculations particularly challenging, leaving total synthesis of the target compound as the only way to elucidate the undetermined C8 stereochemistry. By employing the analogous synthetic route presented in Scheme 3, we synthesized both structural candidates of elodeoidin B, **2a** and **2b**, from (*S*)-2-methylbutanal (**45**) and (*R*)-2-methylbutanal (**46**), respectively (Scheme 7). ^{1}H NMR analysis of synthetic (−)-(8*S*)-

Scheme 7. Total synthesis of (−)-(8*S*)-Elodeoidin B (2a) and (−)-(8*R*)-Elodeoidin B (2b) and Stereochemical Assignment of Elodeoidin B Based on ^{1}H NMR Spectral Analysis of Synthetic 2a and 2b and Natural Elodeoidin B

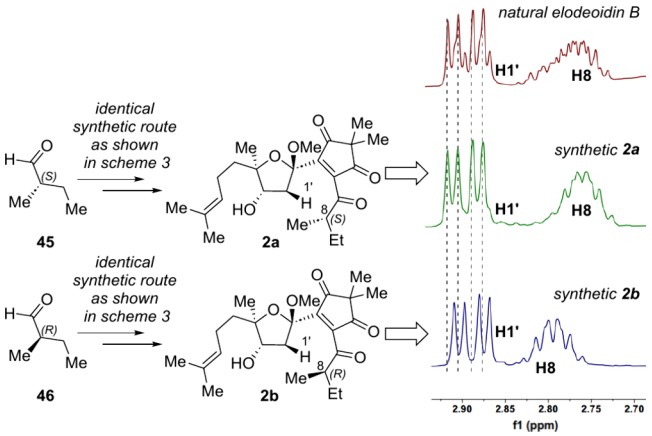

elodeoidin B (**2a**), (−)-(8*R*)-elodeoidin B (**2b**), and natural elodeoidin B revealed that the natural product exists as a mixture of epimers at the C8 stereocenter. The natural sample of elodeoidin B contains (−)-(8*S*)-elodeoidin B (**2a**) as the major component, with (−)-(8*R*)-elodeoidin B (**2b**) present as the minor epimer.

In conclusion, we have achieved a convergent total synthesis of elodeoidins A (**1**) and B (**2**) using a CDC reaction between an aldehyde and an electron-deficient olefin. The key CDC reaction, involving aldehyde **13** and enetrione coupling partner **20**, was catalyzed by $Cu(dap)_2PF_6$ and utilized TBPB as an oxidant under 525 nm green light irradiation. DFT calculations revealed that the reaction mechanism, enabled by these newly developed conditions, involves concerted deprotonation within the transient formal Cu(III) complex. Moreover, the total synthesis of both structural candidates of elodeoidin B demonstrated that natural elodeoidin B exists as a mixture of diastereomers at the C8 stereocenter. Ongoing research is focused on applying the newly developed CDC reaction to the synthesis of other natural products, which will be detailed in future reports.

■ ASSOCIATED CONTENT

Supporting Information

The Supporting Information is available free of charge at https://pubs.acs.org/doi/10.1021/jacsau.5c00201.

Experimental procedures, detailed optimization studies, characterization data (^{1}H, and ^{13}C NMR, and HRMS), and copies of NMR spectra of new compounds (PDF)

■ AUTHOR INFORMATION

Corresponding Authors

Sunkyu Han − *Department of Chemistry, Korea Advanced Institute of Science & Technology (KAIST), Daejeon 34141, Republic of Korea; Center for Multiscale Chiral Architectures (CMCA), KAIST, Daejeon 34141, Republic of Korea;* orcid.org/0000-0002-9264-6794; Email: sunkyu.han@kaist.ac.kr

Yoonsu Park − *Department of Chemistry, Korea Advanced Institute of Science & Technology (KAIST), Daejeon 34141, Republic of Korea;* orcid.org/0000-0003-1511-0635; Email: yoonsu.park@kaist.ac.kr

Authors

Chungwoo Lee − *Department of Chemistry, Korea Advanced Institute of Science & Technology (KAIST), Daejeon 34141, Republic of Korea; Center for Multiscale Chiral Architectures (CMCA), KAIST, Daejeon 34141, Republic of Korea;* orcid.org/0000-0002-8167-0297

Gyumin Kang − *Department of Chemistry, Korea Advanced Institute of Science & Technology (KAIST), Daejeon 34141, Republic of Korea; Center for Multiscale Chiral Architectures (CMCA), KAIST, Daejeon 34141, Republic of Korea*

Jaehyun You − *Department of Chemistry, Korea Advanced Institute of Science & Technology (KAIST), Daejeon 34141, Republic of Korea;* orcid.org/0000-0002-5736-939X

Taewan Kim − *Department of Chemistry, Korea Advanced Institute of Science & Technology (KAIST), Daejeon 34141, Republic of Korea; Center for Multiscale Chiral Architectures (CMCA), KAIST, Daejeon 34141, Republic of Korea*

Hee-Seung Lee − *Department of Chemistry, Korea Advanced Institute of Science & Technology (KAIST), Daejeon 34141, Republic of Korea; Center for Multiscale Chiral Architectures (CMCA), KAIST, Daejeon 34141, Republic of Korea;* orcid.org/0000-0003-0004-1884

Complete contact information is available at: https://pubs.acs.org/10.1021/jacsau.5c00201

Notes

The authors declare no competing financial interest.

■ ACKNOWLEDGMENTS

We thank Dr. Jeonguk Kweon (IBS), Dr. Joon Heo (SAIT), Dr. Bohyun Park (Samsung Electronics), and Dr. Seongyeon Kwon (IBS) for constructive discussions and guidance with computational studies including IBO analysis. We thank Prof. Jun Luo (China Pharmaceutical University) for providing us with NMR data of the natural elodeoidin B. We thank Chiral Technology Korea and Daicel Chiral Technologies (China) for

their assistance with chiral HPLC. This work was supported by the National Research Foundation of Korea (NRF) grant funded by the Korean government (MSIT) (NRF-2021R1A2C2011203, NRF-2018R1A5A1025208) and by the BK21 FOUR Project. This research was also supported by KAIST Cross-Generation Collaborative Lab Project.

REFERENCES

(1) Yang, X.-W.; Grossman, R. B.; Xu, G. Research Progress of Polycyclic Polyprenylated Acylphloroglucinols. *Chem. Rev.* **2018**, *118*, 3508−3558.
(2) Xie, J.-Y.; Li, P.; Yan, X.-T.; Gao, J.-M. Discovery from *Hypericum elatoides* and synthesis of hyperelanitriles as α-amino-propionitrile-containing polycyclic polyprenylated acylphloroglucinols. *Commun. Chem.* **2024**, *7*, 1.
(3) Li, Q.-J.; Tang, P.-F.; Zhou, X.; Lu, W.-J.; Xu, W.-J.; Luo, J.; Kong, L.-Y. Dimethylated acylphloroglucinol meroterpenoids with anti-oral-bacterial and anti-inflammatory activities from *Hypericum elodeoides*. *Bioorg. Chem.* **2020**, *104*, 104275.
(4) Mu, Y.; Li, Y.; Li, Q.; Xu, W.; Sun, Y.; Wang, S.; Cui, L.; Kong, L.; Luo, J. Elodexanthones A—J, Isoprenylated Xanthone Derivatives with Diverse Skeletons and Bioactivities from *Hypericum elodeoides*. *Chin. J. Chem.* **2022**, *40*, 2939−2946.
(5) Grenning, A. J.; Boyce, J. H.; Porco, J. A., Jr Rapid Synthesis of Polyprenylated Acylphloroglucinol Analogs via Dearomative Conjunctive Allylic Annulation. *J. Am. Chem. Soc.* **2014**, *136*, 11799−11804.
(6) Jang, D.; Choi, M.; Chen, J.; Lee, C. Enantioselective Total Synthesis of (+)-Garsubellin A. *Angew. Chem., Int. Ed.* **2021**, *60*, 22735−22739.
(7) Samkian, A. E.; Virgil, S. C.; Stoltz, B. M. Total Synthesis of Hypersampsone M. *J. Am. Chem. Soc.* **2024**, *146*, 18886−18891.
(8) Lam, H. C.; Spence, J. T. J.; George, J. H. Biomimetic Total Synthesis of Hyperjapones A−E and Hyperjaponols A and C. *Angew. Chem., Int. Ed.* **2016**, *55*, 10368−10371.
(9) Li, Q.-J.; Tang, P.-F.; Zhou, X.; Lu, W.-J.; Xu, W.-J.; Luo, J.; Kong, L.-Y. Elodeoidins A−H, acylphloroglucinol meroterpenoids possessing diverse rearranged skeletons from *Hypericum elodeoides*. *Org. Chem. Front.* **2021**, *8*, 1409−1414.
(10) Yang, X.-W.; Li, Y.-P.; Su, J.; Ma, W.-G.; Xu, G. Hyperjapones A−E, Terpenoid Polymethylated Acylphloroglucinols from *Hypericum japonicum*. *Org. Lett.* **2016**, *18*, 1876−1879.
(11) Bao, R.; Zhang, H.; Tang, Y. Biomimetic Synthesis of Natural Products: A Journey To Learn, To Mimic, and To Be Better. *Acc. Chem. Res.* **2021**, *54*, 3720−3733.
(12) Chapman, O. L.; Engel, M. R.; Springer, J. P.; Clardy, J. C. The Total Synthesis of Carpanone. *J. Am. Chem. Soc.* **1971**, *93*, 6696−6698.
(13) Godfrey, R. C.; Green, N. J.; Nichol, G. S.; Lawrence, A. L. Total synthesis of brevianamide A. *Nat. Chem.* **2020**, *12*, 615−619.
(14) French, S. A.; Sumby, C. J.; Huang, D. M.; George, J. H. Total Synthesis of Atrachinenins A and B. *J. Am. Chem. Soc.* **2022**, *144*, 22844−22849.
(15) Lee, S.; Kang, G.; Chung, G.; Kim, D.; Lee, H.-Y.; Han, S. Biosynthetically Inspired Syntheses of Secu′amamine A and Fluvirosaones A and B. *Angew. Chem., Int. Ed.* **2020**, *59*, 6894−6901.
(16) Seong, S.; Lim, H.; Han, S. Biosynthetically Inspired Transformation of Iboga to Monomeric Post-iboga Alkaloids. *Chem.* **2019**, *5*, 353−363.
(17) Li, X.-Y.; Zhang, L.-J.; Yang, Y.-Y.; Lu, W.-J.; Ye, S.-T.; Zhang, H.; Kong, L.-Y.; Xu, W.-J. Isolation and Biomimetic Semisynthesis of Hyperzrones A and B, Two Nor-Polycyclic Polyprenylated Acylphloroglucinols with a Characteristic Cyclobutane Moiety, from *Hypericum beanie*. *Org. Lett.* **2024**, *26*, 10964−10969.
(18) Liu, C.; Yuan, J.; Gao, M.; Tang, S.; Li, W.; Shi, R.; Lei, A. Oxidative coupling between two hydrocarbons: An update of recent C−H functionalizations. *Chem. Rev.* **2015**, *115*, 12138−12204.
(19) Li, C.-J. Cross-Dehydrogenative Coupling (CDC): Exploring C−C Bond Formations beyond Functional Group Transformations. *Acc. Chem. Res.* **2009**, *42*, 335−344.
(20) Shi, Z.; Schröder, N.; Glorius, F. Rhodium(III)-Catalyzed Dehydrogenative Heck Reaction of Salicylaldehydes. *Angew. Chem., Int. Ed.* **2012**, *51*, 8092−8096.
(21) Niu, B.; Xu, L.; Xie, P.; Wang, M.; Zhao, W.; Pittman, C. U., Jr; Zhou, A. Diversity-Oriented Syntheses: Coupling Reactions Between Electron-Deficient Olefins and Aryl Aldehydes via $C(sp^2)$−H Functionalization. *ACS Comb. Sci.* **2014**, *16*, 454−458.
(22) Adib, M.; Pashazadeh, R.; Rajai-Daryasarei, S.; Kabiri, R.; Jahani, M. Transition metal-free cross-dehydrogenative coupling acylation of coumarins by the $K_2S_2O_8$/Aliquat 336 catalytic system: a versatile strategy towards 4-aroylcoumarin derivatives. *RSC Adv.* **2016**, *6*, 110656−110660.
(23) Borah, A.; Sharma, A.; Hazarika, H.; Gogoi, P. Synthesis of 2,3-Disubstituted 1,4-Naphthoquinones via Metal-Free C(sp2)-H Functionalization Followed by Suzuki Cross-Coupling Reactions. *ChemistrySelect* **2017**, *2*, 9999−10003.
(24) Kang, G.; Han, S. Synthesis of Dimeric Securinega Alkaloid Flueggeacosine B: From Pd-Catalyzed Cross-Coupling to Cu-Catalyzed Cross-Dehydrogenative Coupling. *J. Am. Chem. Soc.* **2022**, *144*, 8932−8937.
(25) Han, S. "K-synthesis": Recent advancements in natural product synthesis enabled by unique methods and strategies development in Korea. *Bull. Korean Chem. Soc.* **2023**, *44*, 172−201.
(26) Pirtsch, M.; Paria, S.; Matsuno, T.; Isobe, H.; Reiser, O. $[Cu(dap)_2Cl]$ As an Efficient Visible-Light-Driven Photoredox Catalyst in Carbon−Carbon Bond-Forming Reactions. *Chem. Eur. J.* **2012**, *18*, 7336−7340.
(27) Kuwana, D.; Nagatomo, M.; Inoue, M. Total Synthesis of 5-*epi*-Eudesm-4(15)-ene-1β,6β-diol via Decarbonylative Radical Coupling Reaction. *Org. Lett.* **2019**, *21*, 7619−7623.
(28) Yamano, Y.; Nishiyama, Y.; Aoki, A.; Maoka, T.; Wada, A. Total synthesis of lycopene-5,6-diol and γ-carotene-5′,6′-diol stereoisomers and their HPLC separation. *Tetrahedron* **2017**, *73*, 2043−2052.
(29) Tsunoda, T.; Suzuki, M.; Noyori, R. A facile procedure for acetalization under aprotic conditions. *Tetrahedron Lett.* **1980**, *21*, 1357−1358.
(30) Esposti, S.; Dondi, D.; Fagnoni, M.; Albini, A. Acylation of Electrophilic Olefins through Decatungstate-Photocatalyzed Activation of Aldehydes. *Angew. Chem., Int. Ed.* **2007**, *46*, 2531−2534.
(31) Gorbachev, D.; Smith, E.; Argent, S. P.; Newton, G. N.; Lam, H. W. Synthesis of New Morphinan Opioids by TBADT-Catalyzed Photochemical Functionalization at the Carbon Skeleton. *Chem. Eur. J.* **2022**, *28*, e202201478.
(32) Rawner, T.; Lutsker, E.; Kaiser, C. A.; Reiser, O. The different faces of photoredox catalysts: Visible-light-mediated atom transfer radical addition (ATRA) reactions of perfluoroalkyl iodides with styrenes and phenylacetylenes. *ACS Catal.* **2018**, *8*, 3950−3956.
(33) Engl, S.; Reiser, O. Copper makes the difference: Visible light-mediated atom transfer radical addition reactions of iodoform with olefins. *ACS Catal.* **2020**, *10*, 9899−9906.
(34) Cismesia, M. A.; Yoon, T. P. Characterizing chain processes in visible light photoredox catalysis. *Chem. Sci.* **2015**, *6*, 5426−5434.
(35) Jang, Y. J.; An, H.; Choi, S.; Hong, J.; Lee, S. H.; Ahn, K.-H.; You, Y.; Kang, E. J. Green-light-driven $Fe(III)(btz)_3$ photocatalysis in the radical cationic [4 + 2] cycloaddition reaction. *Org. Lett.* **2022**, *24*, 4479−4484.
(36) Beckwith, A. L. J.; Zavitsas, A. A. Allylic oxidations by peroxy esters catalyzed by copper salts. The potential for stereoselective syntheses. *J. Am. Chem. Soc.* **1986**, *108*, 8230−8234.
(37) Andrus, M. B.; Argade, A. B.; Chen, X.; Pamment, M. G. The asymmetric kharasch reaction. Catalytic enantioselective allylic acyloxylation of olefins with chiral copper(I) complexes and *tert*-butyl perbenzoate. *Tetrahedron Lett.* **1995**, *36*, 2945−2948.
(38) Xu, J.; Fu, Y.; Luo, D.-F.; Jiang, Y.-Y.; Xiao, B.; Liu, Z.-J.; Gong, T.-J.; Liu, L. Copper-catalyzed trifluoromethylation of terminal

https://doi.org/10.1021/jacsau.5c00201
JACS Au 2025, 5, 1096−1103

alkenes through allylic C−H bond activation. *J. Am. Chem. Soc.* **2011**, *133*, 15300−15303.
(39) Beniazza, R.; Molton, F.; Duboc, C.; Tron, A.; McClenaghan, N. D.; Lastécouères, D.; Vincent, J.-M. Copper(I)-photocatalyzed trifluoromethylation of alkenes. *Chem. Commun.* **2015**, *51*, 9571−9574.
(40) Wang, P.-Z.; Wu, X.; Cheng, Y.; Jiang, M.; Xiao, W.-J.; Chen, J.-R. Photoinduced copper-catalyzed asymmetric three-component coupling of 1,3-dienes: An alternative to Kharasch-Sosnovsky reaction. *Angew. Chem., Int. Ed.* **2021**, *60*, 22956−22962.
(41) Kern, J.-M.; Sauvage, J.-P. Photoassisted C−C coupling via electron transfer to benzylic halides by a bis(di-imine) copper(I) complex. *J. Chem. Soc., Chem. Commun.* **1987**, *8*, 546−548.
(42) Baron, R.; Darchen, A.; Hauchard, D. Electrode reaction mechanisms for the reduction of *tert*-butyl peracetate, lauryl peroxide and dibenzoyl peroxide. *Electrochim. Acta* **2006**, *51*, 1336−1341.
(43) Kochi, J. K.; Bemis, A.; Jenkins, C. L. Mechanism of electron transfer oxidation of alkyl radicals by copper(II) complexes. *J. Am. Chem. Soc.* **1968**, *90*, 4616−4625.
(44) Chen, M.; Dong, G. Copper-Catalyzed Desaturation of Lactones, Lactams, and Ketones under pH-Neutral Conditions. *J. Am. Chem. Soc.* **2019**, *141*, 14889−14897.
(45) Liu, S.; Liao, Y.; Li, H.; Xu, B.; Zhang, X.; Shang, Y.; Su, W. Straightforward α-allylation of carbonyl compounds with alkenes *via* α-carbonyl radical intermediates. *Org. Chem. Front.* **2024**, *11*, 2502−2511.
(46) Hossain, A.; Engl, S.; Lutsker, E.; Reiser, O. Visible-Light-Mediated Regioselective Chlorosulfonylation of Alkenes and Alkynes: Introducing the Cu(II) Complex [Cu(dap)Cl_2] to Photochemical ATRA Reactions. *ACS Catal.* **2019**, *9*, 1103−1109.
(47) Knizia, G.; Klein, J. E. M. N. Electron Flow in Reaction Mechanisms—Revealed from First Principles. *Angew. Chem., Int. Ed.* **2015**, *54*, 5518−5522.
(48) Kang, G.; Baik, M.-H.; Han, S. Calculation-Assisted Stereochemical Analysis of Securingine A. *Bull. Korean Chem. Soc.* **2021**, *42*, 486−488.
(49) Kim, T.; Kim, S.; Chung, G.; Park, K.; Han, S. Re-examining the stereochemistry of polycyclic suffruticosine *via* TDDFT calculations, ECD spectroscopy, and chemical synthesis. *Org. Chem. Front.* **2023**, *10*, 5123−5129.
(50) Kim, S.; Park, I.; Kim, M.; Lee, G. S.; Kim, C. S.; Han, S. Synthesis and Structure Revision of Securingine E. *Org. Lett.* **2024**, *26*, 7166−7169.

https://doi.org/10.1021/jacsau.5c00201
JACS Au 2025, 5, 1096−1103